Prefeasibility mining studies by using electrical resistivity imaging (ERI) in Keratong, Pahang

Puteri Izrina Ismi, Mohd Fakhrurrazi Ishak*, Solahuddin Daud

Faculty of Civil Engineering Technology, Universiti Malaysia Pahang Al-Sultan Abdullah, Lebuh Persiaran Tun Khalil Yaakob, Kampung Melayu Gambang, 26300 Kuantan, Pahang, Malaysia *Corresponding author email address: fakhrurrazi@umpsa.edu.my

Abstract: The allure of hidden mineral wealth has long driven exploration yet the complexity of uncovering these resources beneath layers of the earth's surface remains a formidable challenge. In Keratong, Pahang, a geophysical investigation employing electrical resistivity imaging (ERI) was conducted to map the intricate subsurface landscape across a 1.25 km^2 of a study area. Eight survey lines were meticulously analysed using a combination of resistivity and induced polarization techniques thus culminating in vivid 2D pseudo-sections and a dynamic 3D contour model. These visualisations reveal a stratified geological profile comprising of overburdened soil, weathered metasediments, and fractured sedimentary rocks that obscure the presence of potential metallic mineral deposits. Notably, zone exhibiting low resistivity (0–40 Ω m) and high chargeability (>240 ms) suggest the presence of mineralization at depths ranging from 5 to 20 meters, particularly along Line 2, 4, 5, 6, 7, and 8. The northwest region, identified as suitable for tailing ponds, mine facilities, and stable terrain near Line 1 and 3 is recommended for stockpiling while demonstrating an integrated approach for exploration and sustainable site planning. This research underscores the transformative potential of ERI in both location subsurface mineral resources and stating the design efficiency for environmentally responsible mining operations.

Keywords: Electrical resistivity imaging (ERI), precious mineral exploration, hematite ore, 2D and 3D modelling, geophysical survey

HIGHLIGHTS

Geophysical Survey Application: Conducted ERI on eight survey lines covering a 1.25 km² area in Keratong, Pahang using resistivity and chargeability data to characterize subsurface conditions and to locate potential ore bodies.

Subsurface Visualization: Developed 2D pseudosections and 3D contour models, enabling detailed analysis of overburden soil, weathered metasediments, and fractured sedimentary rock formations.

Mineralization Insights: Identified low resistivity $(0-40~\Omega m)$ and high chargeability (>240 ms) zones indicating metallic mineral deposits with significant findings on Line 2, 4, 5, 6, 7, and 8 at depths of 5 to 20 meters.

Site Recommendations: Proposed borehole drilling at key mineralized zones and suggested optimal locations for tailing ponds in the northwest and mine facilities in stable and elevated terrain.

Efficient Mine Development: The results provide a comprehensive framework for mineral extraction, site planning, and infrastructure placement while minimizing environmental and operational risks.

INTRODUCTION

The wide application of minerals in daily life has caused their demand to soar, driving the technological advancement and development of high-tech innovations. A mineral orebody refers to a naturally formed inorganic substances with unique chemical compositions, distinct crystalline structure and specific physical properties. These deposits contain economically valuable concentrations of one or more minerals, such as gold, tin, iron, and silver, which can be extracted and sold at a profit (Misra, 1999). Minerals are fundamental to a wide range of industries, such as manufacturing, construction, agriculture, energy supply, and more. However, as mineral ore bodies are typically located beneath the earth surface and scattered across the globe, their extraction poses challenges. To meet rising demands, mining industry stakeholders continue to invest on substantial time and financial resources into mineral exploration.

In the life cycle of mining, mineral exploration represents the upstream stage, usually conducted by a group of certified geologists. According to Haldar (2018), the

initial stage of identifying the potential minerals within a regional scale is referred to as reconnaissance or grassroots exploration. This phase involves both direct techniques, such as physical geological mapping and indirect techniques, including geochemical testing (Tan *et al.*, 2018). Common early-stage activities including literature review, geological site visits, and geochemical testing were conducted to assess the mineral potential for future mining operations. However, these preliminary studies alone are often insufficient to accurately identify subsurface anomalies or for analyzing, evaluating, and predicting geological conditions in two and three dimensions.

Geophysical surveys play a vital role in investigating and characterizing subsurface geology by detecting variations in material properties at depth, without the need for borehole drilling (Zaini et al., 2019; Kearey et al., 2002). These methods are cost effective, rapid, and capable of covering large areas, making them a preferred choice in mineral exploration (Zaini et al., 2019; Kearey et al., 2002; Zaid et al., 2022; Zaid et al., 2023). Several geophysical techniques are commonly employed, including seismic method, magnetic survey, electrical resistivity imaging (ERI), gravity survey, and induced polarization (IP) methods. Each technique measures different geophysical parameters based on specific physical properties (Bery et al., 2011). The key parameter measured in ERI is the earth's resistance, while its operative physical property is electrical conductivity. The outcomes of ERI surveys are typically presented in two-dimensional (2D) visualizations, allowing for efficient and precise subsurface interpretation. Consequently, geophysical survey methods are selected to facilitate the visualization of mineral distribution in mine prefeasibility study. As reconnaissance exploration progresses, the survey area becomes more focused on regions with elevated mineral potential. At the end of the research, the geophysical findings also support the planning of borehole drilling for further feasibility studies.

Moreover, mine development is a continous process within the mine life cycle. In the early development, pit planning is essential to keep the cost to the minimum. It includes a land rehabilitation plan as part of an environmental impact statement (EIS), as well as designing mine facilities, topsoil stockpile areas, and waste storage sites. Through geophysical investigations, the conception of the mining area within the study area is conceivable. This paper then aims to locate mineral orebodies in the subsurface, developing a borehole drilling plan, and conducting an initial mine development strategy based on electrical resistivity imaging (ERI) results in Keratong, Pahang. According to Kearey *et al.* (2002) and Arifin *et al.* (2019), ERI is recognized as an effective method for achieving these objectives.

GEOLOGICAL SETTING

Due to the confidential agreement, the exact location cannot be disclosed to the public. However, the study area is generally within Keratong, which is located in the Rompin district of Pahang, Peninsular Malaysia. The stratigraphic and structural differences divided Peninsular Malaysia into 3 belts: The Western Belt, Central Belt, and Eastern Belt (Pour & Hashim, 2015). According to the geological map produced by Yamusa *et al.* (2021), Keratong is situated within the central belt of Peninsular Malaysia. Figure 1 shows the Map of Peninsular Malaysia displaying the three (3) belts and the north-western (NW) domain within the Western Belt.

The Bentong-Raub Suture Zone borders the Central Belt to the west while the Lebir Fault Zone lies to the east. This belt is predominantly composed of Permo-Triassic, low-grade metasedimentary rocks, bottomless to shallow marine clastic sediments, and limestone with abundant of intermediate to acid volcanic and volcaniclastics deposited in a paleo-arc basin (Pour & Hashim, 2015). During the Middle to Late Triassic, Semantan formation is distributed mainly in the study area within the Central Belt (Mohamed & Abdullah, 1993). This formation consists of a "rapidly alternating sequence of carbonaceous shale, siltstone, and tuffaceous sandstone, with a few lenses of conglomerate and limestone. The shale and tuffaceous sandstone make up the bulk of the sequences," as mentioned by Mohamed & Abdullah (1993) and Peng et al. (2004). This subject also agrees with Hutchison & Tan (2009), who mentioned in their study that deeper marine turbidity sediments, commonly tuffaceous and occasionally interbedded with volcanic material, are part of Semantan formation. The formation is further subdivided into argillaceous, pyroclastic, limestone, and chert facies with no timestratigraphic significance (Peng et al., 2004; Sajid et al., 2020). The rock sequence in Felda Keratong 8 exhibits a typical fining-upward pattern, primarily comprising fine to coarse-grained cross-bedded sandstone, parallel-laminated siltstone, and mudstone. This sequence has been identified as the Gerek Formation (Cook & Suntharalingam, 1970) and is interpreted to be originated from sedimentation within a fluvial depositional environment as described in detail by Said (2002). Figure 2 shows the outcrop of the study area.

ELECTRICAL RESISTIVITY IMAGING (ERI)

ERI (Electrical resistivity imaging) is an integrated approach that combines electrical surveying, resistivity methods, and data modelling to generate visual representations in both 2D and 3D formats. This non-destructive technique ensures minimal disruption and damage to the surveyed site (Syakir *et al.*, 2020). A few benefits of this is from naturally occurring electric fields within the earth, while the others need the introduction of artificial—generated current into the ground (Kearey *et al.*, 2002; Haldar, 2018). The electric current is propagated through a pair of electrodes injected into the ground and through any inhomogeneous conditions in the presence of an electrically conductive or resistive object (Haldar, 2018).

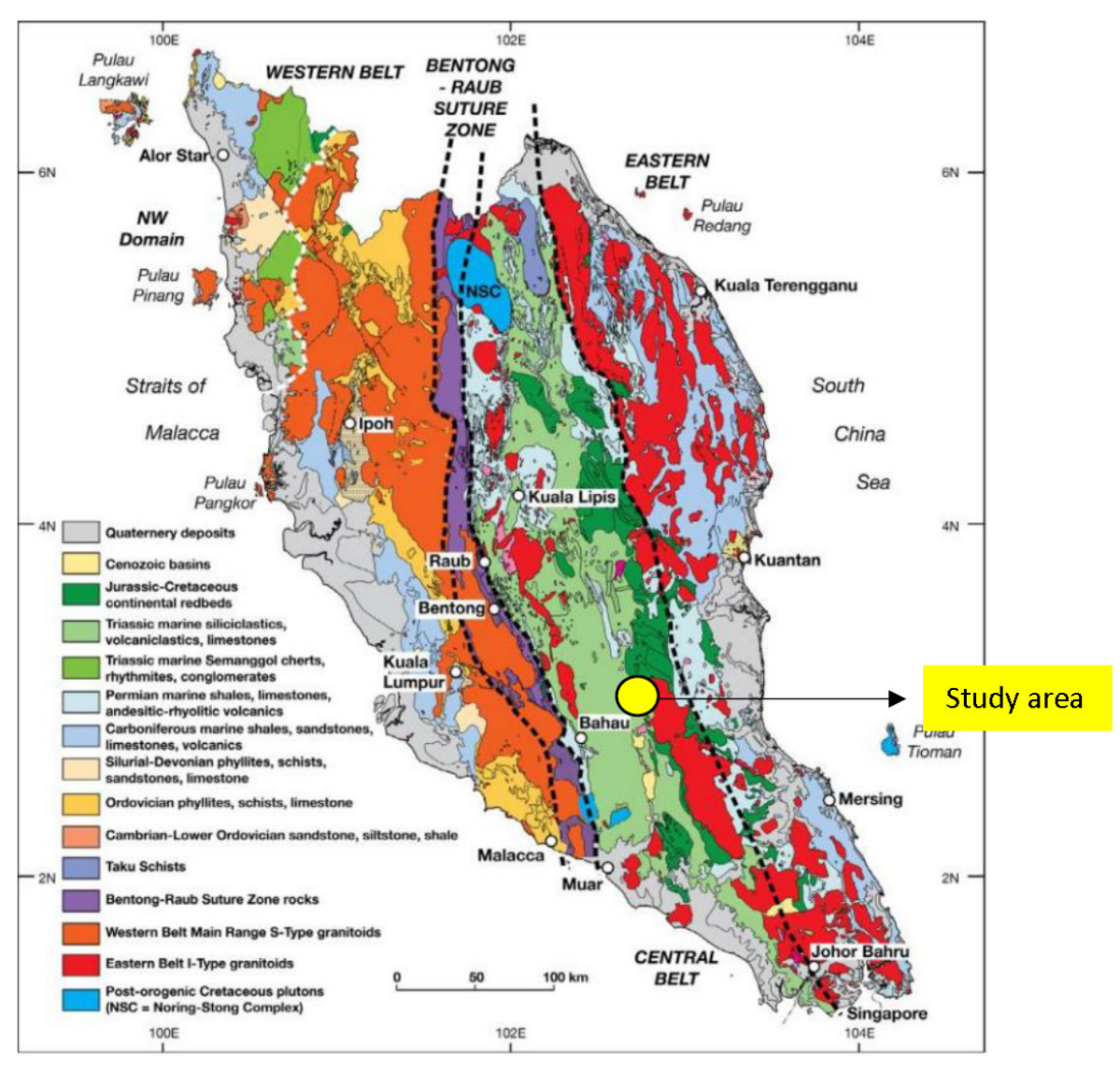


Figure 1: The simplified geological map of Peninsular Malaysia. The yellow circle indicates the study area. Source: Yamusa *et al.* (2021).



Figure 2: The outcrop of the study area.

Resistivity is the resistance (ohm) between the opposite faces of a unit cube of the material (Kearey *et al.*, 2002; Haldar, 2018; Jones, 2018). This method injected the artificial-generated electric current into the ground, and the potential difference (volts) was measured (Wightman *et al.*, 2004; Nordiana *et al.*, 2012; Haldar, 2018). The standard method of measuring electrical resistivity is through a four-electrode measurement in which 2 electrodes act as current electrodes, injecting the current and the other 2 act as potential electrodes, measuring the difference of voltage when passing through a resistance. Figure 3 below shows the basic arrangement of the resistivity method.

During the field survey, a multiple–electrode array system will be implemented to enable faster data acquisition over a large area with minimal equipment reconfiguration (Martínez-Pagán *et al.*, 2021). The most common multiple–electrode array systems are Wenner, Schlumberger, and dipole-dipole array. According to Martínez-Pagán *et al.* (2021), the chosen array configuration system influences the resolution of data, the maximum depth of investigation, and the signal–to–noise ratio. Thus, choosing the array configuration system according to the objectives is very important.

Electrical resistivity imaging (ERI) has been proven to be effective for metallic ore exploration. Metallic ores are naturally occurring rocks that contain significant quantities of metals or metal compounds, making them viable for commercial extraction. These ores are typically found within igneous and metamorphic rock formations. The primary types of metallic ores include oxides, sulphides, carbonates, and halides. Iron ore is one of the most found compound and is present in various geological formations, each contributing to the different iron-rich ores. ERI can discriminate ore bodies from surrounding rock, making it a cost-efficient alternative to magnetic methods, especially for oxidized deposits (Far et al., 2015). When combined with induced polarization, ERI enhances subsurface structure resolution and correlates well with conductivity data for iron ore exploration (Bery et al., 2011).

A notable case study by Zaini *et al.* (2020) investigated the use of electrical resistivity tomography (ERT) for granite exploration in Johor, Malaysia. The study demonstrated that ERT effectively delineates subsurface structures and

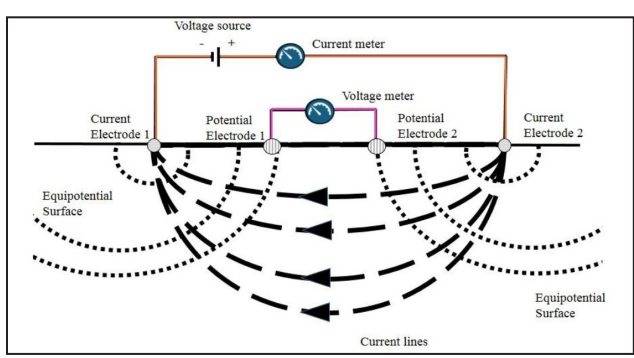


Figure 3: The basic arrangement of the resistivity method.

identified high-resistivity zones indicative of granite, which may be associated with potential mineral deposits. Although primarily focused on granite, the research highlighted the method's broader applicability in near-surface geophysical surveys and its relevance to mineral exploration.

In another instance, Ghoneim *et al.* (2022) applied ERT for iron ore exploration in the Central Eastern Desert of Egypt. Their findings revealed that ERT has successfully mapped resistivity variations linked to hematite and other iron-bearing minerals, facilitating the identification of iron ore deposits. The study emphasized the importance of integrating ERT with geological and geochemical data in order to provide a more comprehensive understanding of subsurface conditions, thereby improving the accuracy of mineral resource assessments.

Similarly, Mielke *et al.* (2016) demonstrated the application of ERT in identifying gossan areas, often linked to hematite deposits, in the Lower Orange River region of South Africa. By combining ERT with remote sensing techniques, the researchers were able to detect iron-bearing minerals, including hematite. Their research underscored the importance of integrating ERT with other geophysical methods to improve the detection and characterization of hematite-rich zones.

A recent study in Nigeria further showcased the capabilities of electrical resistivity imaging (ERI) in detecting the lateral continuity of mineral ore deposits, including magnetite and hematite within the topsoil layer (Layade *et al.*, 2022). However, the study noted a significant variability in the electrical resistivity of ore samples influenced by factors such as ore content and composition. For hematite, resistivity values ranged from 395 Ω m to 6619 Ω m with no clear correlation between resistivity and ore content (Parasnis, 2006; Layade *et al.*, 2022). This variability highlights the importance of combining resistivity data with other techniques for accurate mineral characterization.

Additionally, the study by Yang et al. (2024) highlighted the effectiveness of ERT in mapping alteration zones related to iron oxides. By integrating ERT data with Landsat-8 multispectral imagery, they successfully identified hematiterich zones, further validating the method's applicability in mineral exploration. This integrated approach improved detection capabilities and offers insights into the geological processes driving hematite formation.

2D pseudo-section model and 3D contour model

During the final phase of the electrical resistivity imaging (ERI) process, the development of 2D model views is undertaken. The 2D model aids in visualizing and describing cross-sectional data along the x and y axis during the data analysis. To create the 2D model view, data including the measured and calculated apparent resistivity is used. Initially, the calculated apparent resistivity values are plotted onto a 2D pseudo-section model. Subsequently, an inverse procedure is employed to derive the estimated

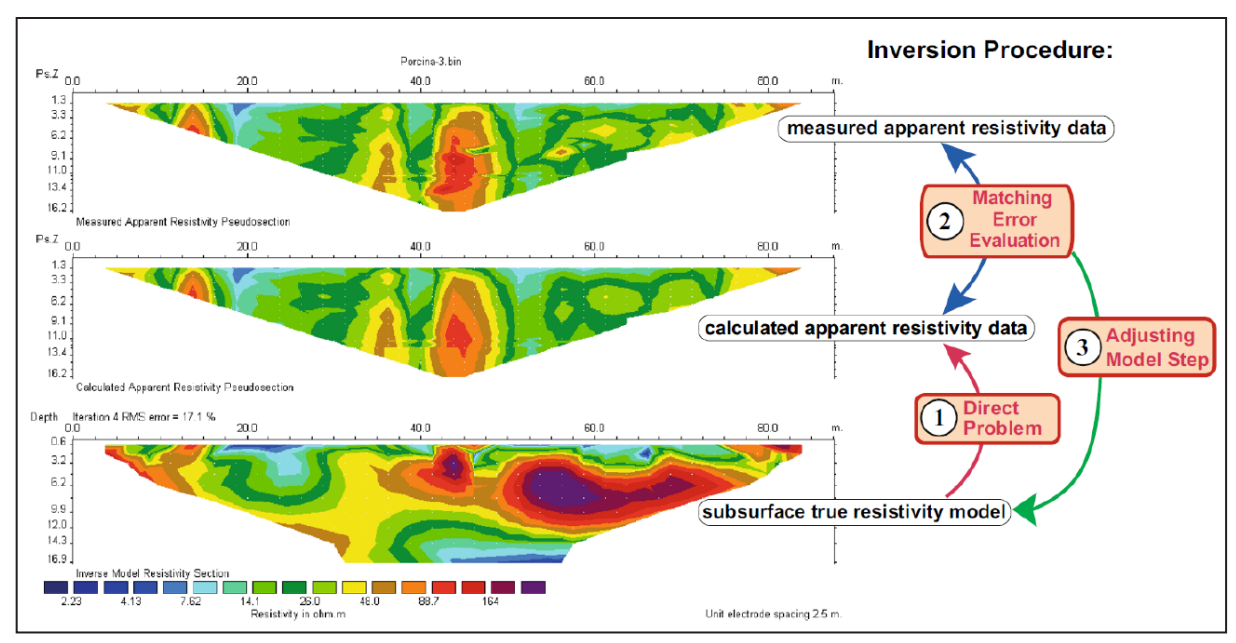


Figure 4: The procedure for modelling 2D model view. Source: Martínez-Pagán et al. (2021).

true resistivity, as the inverted 2D model provides more insight into the natural geological features (Martínez-Pagán *et al.*, 2021). Finally, the model is adjusted iteratively to match the measured resistivity data within an acceptable tolerance closely.

Subsequently, a 3D contour model was developed based on 2D contour graph. The incorporation of a 3D perspective enhances visualisation by providing more sense of depth and nonspatial relationships, enabling more accurate analysis of complex geometries. This, in turn, supports better decision-making by reducing uncertainties in interpretation and facilitating more comprehensive discussion (Yixin *et al.*, 2017). Figure 4 above illustrates the procedure for 2D modelling.

METHODOLOGY

The survey covered about 1.25 km² of an area in a forest, secluded from the public locality. Due to the terrain drawback, the survey lines did not intersect to each other as shown in Figure 5.

ERI surveys were conducted using ABEM Terrameter LS2 with a maximum built-in of 81 internal electrodes and up to 16384 external electrodes connected to it (GuidelineGeo., 2012). Data from the ERI was recorded by Schlumberger protocol. The protocol was chosen due to its good sensitivity to vertical and lateral changes of electrical resistance thus providing high resolution in both directions (Sikah *et al.*, 2016).

To create a two-dimensional (2D) resistivity model of the subsurface, the RES2DINV computer program was utilized with the drawing on the data gathered from electrical imaging surveys (Griffiths & Barker, 1993). The RES2DINV software employs a smooth-constrained method to develop

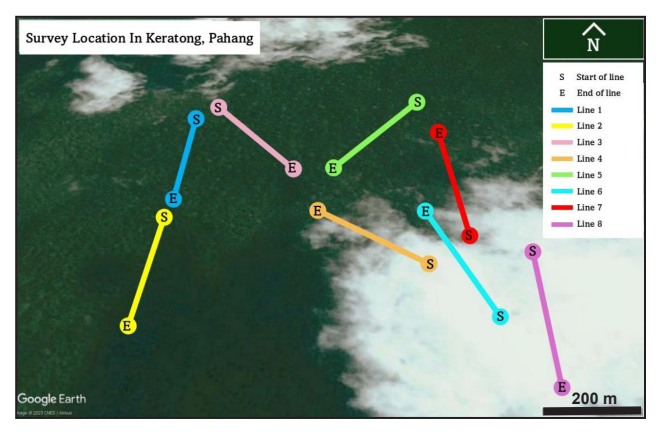


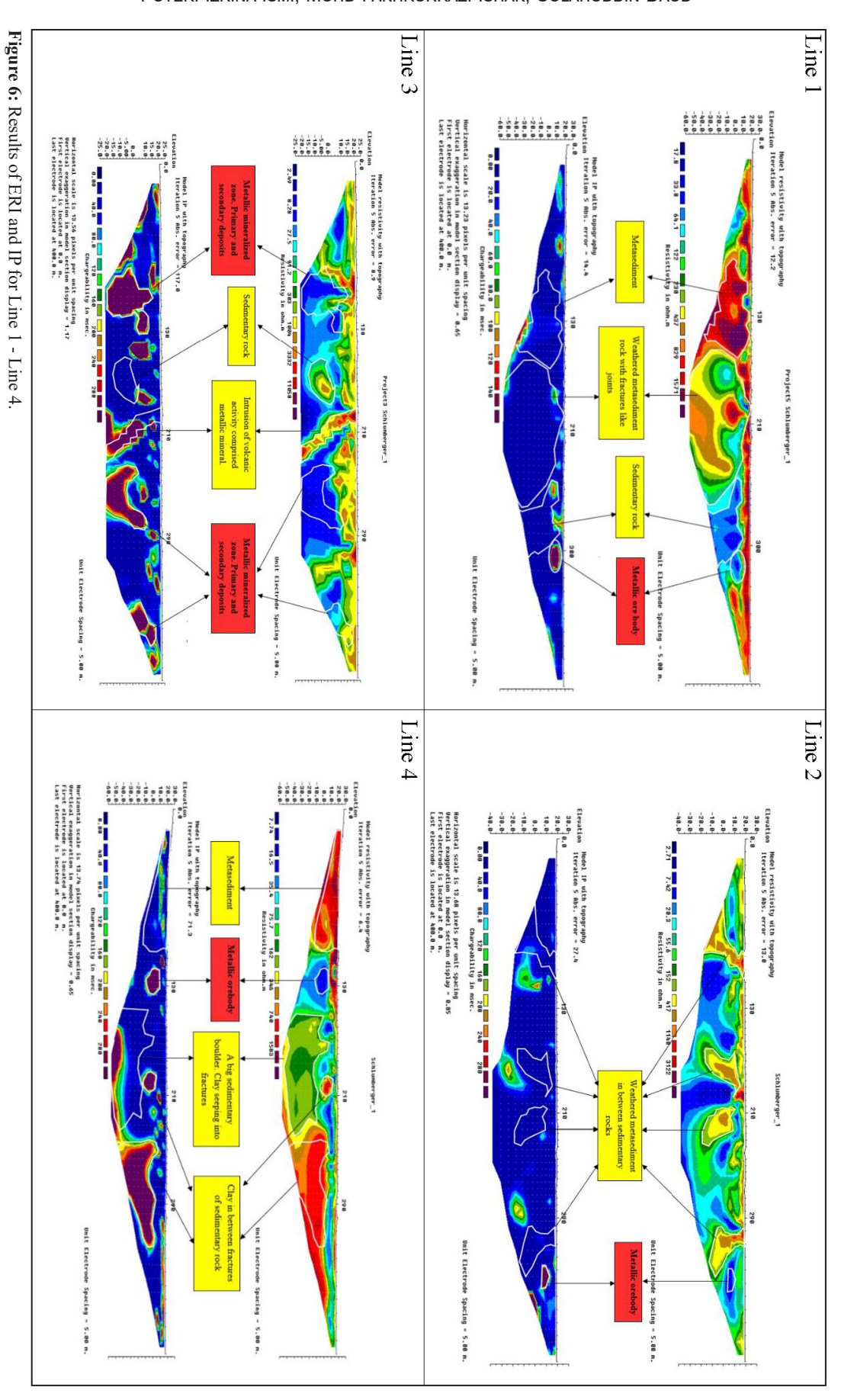
Figure 5: The 8 survey lines within the survey location.

the 2D inverse model, providing a detailed representation of the subsurface profile that closely mimics the actual structure. Subsequently, three-dimensional (3D) contour models were constructed using Surfer software. According to Al-Sudani (2019), Surfer is a powerful software package for contouring, gridding, and surface mapping.

RESULTS

The 2-D inverse model result

Figure 6 and 7 display the 2-D electrical resistivity profiles and the induced polarization (chargeability) data that the RES2DINV software has processed. The geology and subsurface structures in the area were delineated using electrical resistivity data and induced polarization data was utilized to determine the precious mineral orebody (Arifin *et al.*, 2019). Eight electrical resistivity lines were set up within the area of interest as shown in Figure 5. The length of the survey lines is shown on the horizontal scale in meters,



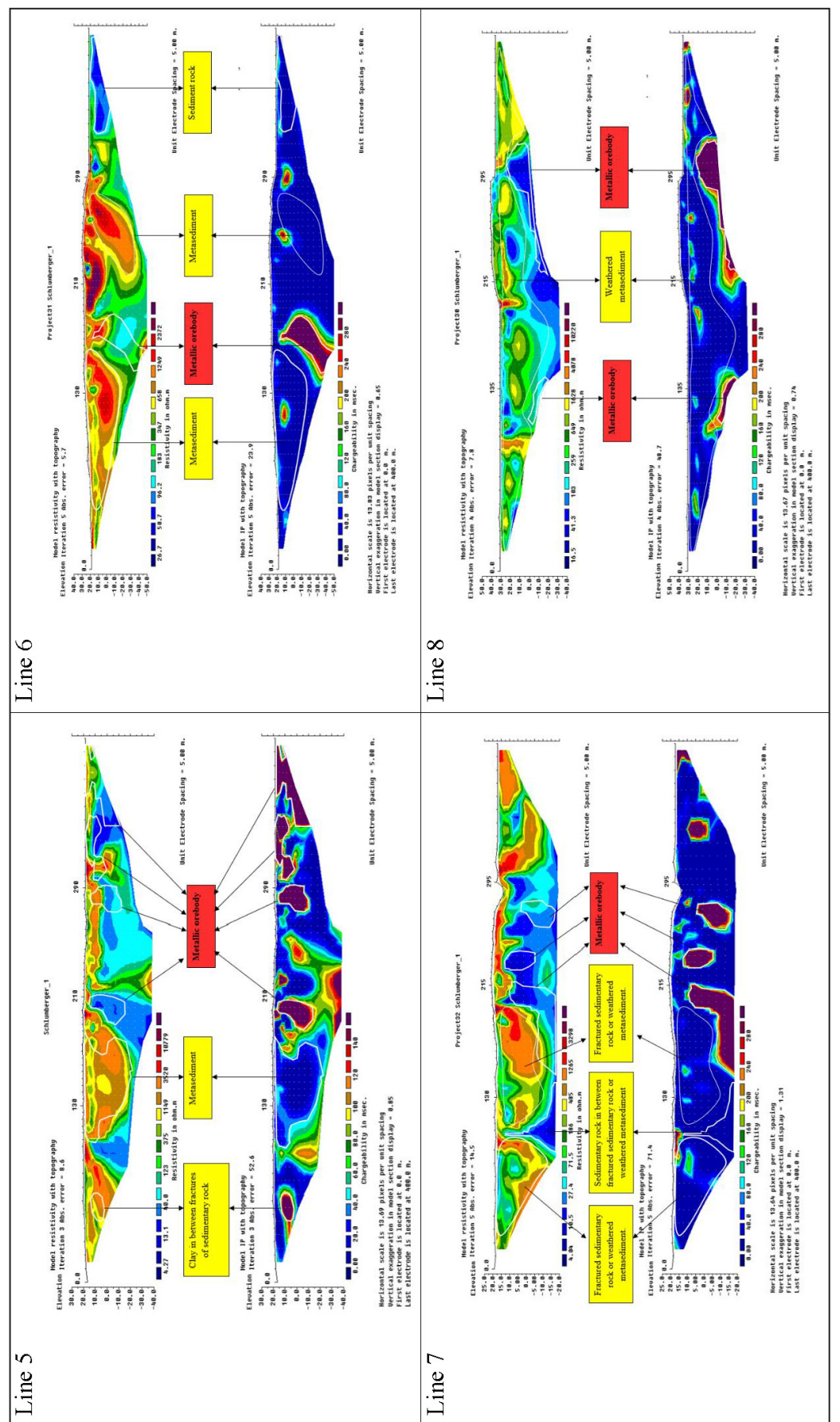


Figure 7: Results of ERI and IP for Line 5 - Line 8.

Table 1: The resistivity value of some common rocks and minerals (Loke, 1999).

Material	Resistivity (ohm / m)					
Igneous and metamorphic rocks						
Granite	5 x 10 ³ - 10 ⁶					
Basalt	10 ³ - 10 ⁶					
Slate	6 x 10 ² - 4 x 10 ⁷					
Marble	10 ² - 2.5 x 10 ⁸					
Quartzite	10 ² - 2 x 10 ⁸					
Hematite Ore	8 - 1 x 10 ⁴					
Magnetite Ore	0.1 - 1 x 10 ³					
Se	dimentary rocks					
Sandstone	8 - 4 x 10 ³					
Shale	20 - 2 x 10 ³					
Limestone	50 - 4 x 10 ²					
;	Soil and water					
Clay	1 - 100					
Alluvium	10 - 800					
Groundwater (fresh)	10 - 100					
Sea water	0.2 - 5					

while the vertical scale in meters represents the elevation. The Schlumberger protocol provided data coverage for the focal point of the survey lines, with maximum depths ranging between 65 to 90 meters. According to Loke (1999), resistivity is highly influenced by the degree of fracturing and the percentage of fractures are filled with groundwater. As a result, igneous and metamorphic rock has a higher resistivity value than sedimentary rock, which is more porous and contain higher water content. Logically, clay with high porosity tends to have much lower resistivity values than sandy soil due to its higher water retention capacity. Materials with the lowest resistivity value are wet soils and fresh water. Table 1 and Table 2 summarize the resistivity value of some common rocks and minerals.

The range of resistivity values varies greatly from 20 Ω m to 5000 Ω m. The color-coding method was applied to represent distinguishing features. At the top side of the ERI 2D inverse profile, a layer of light greenish to reddish colour with resistivity value ranging from 100 Ω m to 1000 Ω m was assumed as overburdened soil. This overburdened soil between 10 to 15 m is comprised of silty sand mixed with organic matter and sand at the stream.

Based on the 2D inverse pseudo-section model, zones with low resistivity values ranging from 0 Ω m to 40 Ω m were represented by bluish colour and that exhibiting high chargeability were interpreted as potential metallic ore bodies. In contrast, zones with high resistivity values ranging from 3000 Ω m to 5000 Ω m shown in reddish tones and assosiated with low chargeability values, were interpreted as metasediment. Furthermore, clay between fractures was

Table 2: Summary of 2D inverse pseudo-section model interpretation code where R: resistivity and C: chargeability.

R	R-Value range (Ωm)	Colour R-value	C	C Value range (msec)	Colour C value	Interpretation
Low	0 - 100	Blue to greenish	High	120 - 300	Reddish – dark purple	Metallic ore bodies
High	1000 - 5000	Reddish – dark purple	Low	0 - 80	Blue to greenish	Metasediment
High	1000 - 5000	Reddish – dark purple	High	120 - 300	Reddish – dark purple	Clay between fractures
Low	0 - 100	Blue to greenish	Low	0 - 80	Blue to greenish	Sedimentary rock
	1200 - 2000	Reddish–dark purple hues				Fractured/jointing metased- iment or sedimentary rock with several orientations of joints.
	100 - 1200	Greenish and yellow-orange hues				Highly fractured zone

construed as having high resistivity values (reddish) and high chargeability (bluish). In addition, sedimentary rock or water is represented by low resistivity values (bluish) and low chargeability values (bluish). Beyond mineral identification, resistivity values between 1200 Ω m and 2000 Ω m depicted in greenish and yellow-orange hues were interpreted as fractured or jointing metasediment or sedimentary rock with multiple orientations of joints. Average resistivity value, ranging from 100 Ω m to 1200 Ω m likely indicate highly fractured zones.

The 3-D contour model result

A 3-D model of the topography map (right) was developed through Surfer software as shown in Figure 8 with a reference to a 2-D topography map (left). Due to the software constraints, only Line 1 until Line 7 can be projected in both topography models. The elevation depicted in both models is measured above sea level, ranging from 17 to 30 meters. The 3D topography model reveals the presence of valleys in the southwest and a hill in the southeast of the study area.

DISCUSSIONS

The ERI conducted as part of the geophysical study has shown promising results in identifying four distinct geological units: 1) overburden soil, 2) metasediment lithology, 3) sedimentary lithology, and 4) potential metallic mineral deposits. The survey area is primarily characterized by sedimentary and metasediment lithology that could be deposited in Permo-Triassic and is associated with fractured or jointed rock properties and covered by a layer of overburdened alluvial or silty sand soil. Low resistivity values (0 Ω m - 40 Ω m) and high chargeability (>240 msec) may suggest the existence of valuable metallic mineral deposits, particularly within the resistivity range associated with hematite ore. Based on the results, most of the hematite bodies are found at the eastern of the survey location. The occurrence of clay may also be inferred from low resistivity and high chargeability readings.

The survey findings reveal diverse geological and mineral potential characteristics across the study area. Line 1 indicates a 10-meter topsoil layer primarily comprising metasediment, sedimentary, and fracture features, with no evidence of metallic minerals. Similarly, Line 3 identifies silty sand topsoil and weathered metasediment, highlighting fractures through resistivity analysis but lacking metallic mineral indications. Line 4 presents a substantial sedimentary boulder at the centre and towards the end of the pseudosection, elevated resistivity and chargeability values suggest clay deposits, while a low-resistivity and high-chargeability zone at 125 meters indicates possible metallic minerals at 10 meters depth. Line 5 highlights potential metallic mineral deposits, both secondary (placer) and primary within the metasediment-dominated lithology at approximately 5 meters depth.

Lines 2, 6, 7, and 8 offer significant mineralization insights. Line 2 reveals a 10-meter topsoil layer with inferred metallic mineral zones at three locations approximately 10 meters below the surface, necessitating further borehole or trial pit investigations. Line 6 identifies a solitary metallic ore deposit,175 meters along the line at a depth of 10 meters. Line 7 points to fractured sedimentary rocks hosting a potential metallic ore deposit at 200 meters and is confirmed by low resistivity and high chargeability values. Line 8, characterized by 10 to 15 meters of alluvial topsoil, indicates two substantial metallic ore deposits at an approximate depth of 20 meters. These findings collectively emphasize the importance of detailed follow-up investigations, including geochemical sampling, borehole drilling, and advanced geophysical surveys to confirm and delineate these potential deposits.

Based on the ERI results above, a borehole drilling plan can be executed efficiently by considering the cost to the minimum. The boreholes should be drilled at locations with potential metallic mineral deposits. On Line 2, specific recommendations including drilling at three identified locations where potential metallic minerals are inferred

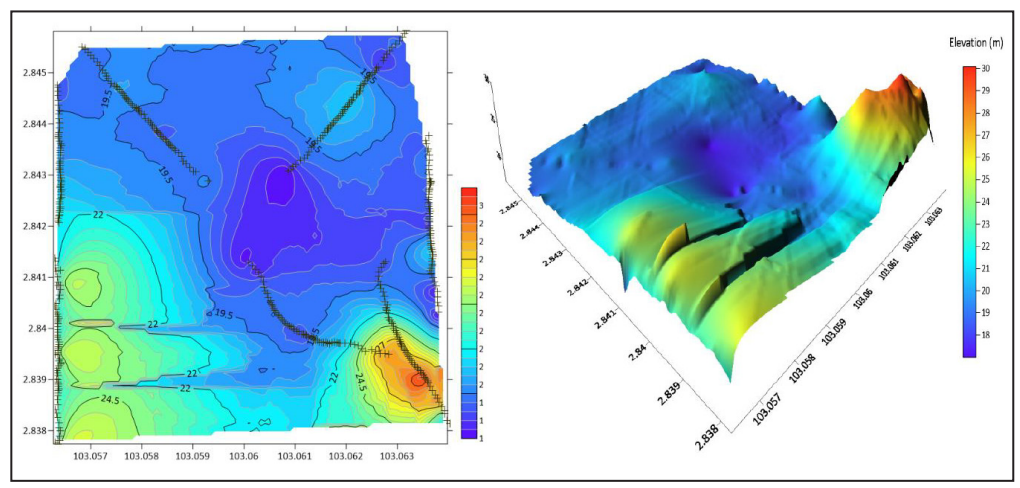


Figure 8: 2D topography map (left) and 3D topography map (right).

at approximately 10 meters below the surface. Boreholes should target these zones as outlined by the resistivity and chargeability data. Furthermore, at Line 4, drilling at 125 meters along the line targeting the low-resistivity and high-chargeability zone which indicates potential metallic minerals at 10 meters depth is suggested and for Line 5, the drilling should be executed in areas showing evidence of secondary (placer) and primary metallic mineral deposits, approximately 5 meters below the surface. In addition, at Line 6, drilling at 175 meters along the line where a solitary metallic ore deposit is suggested at a depth of 10 meters and for Line 7, drilling at 200 meters along the line focusing on the low-resistivity and high-chargeability zone that indicates potential metallic ore can be executed. Lastly, at Line 8, drilling at the two locations where significant metallic ore deposits are inferred at approximately 20 meters depth is suggested. These locations were selected based on the geophysical interpretation of low resistivity and high chargeability values, which are the strong indicators of metallic mineral deposits. Borehole drilling in these zones will provide precise data to confirm the mineralization and support further exploration activities.

The combination of the ERI and contour map results helps in planning the initial mine development, such as the placement of the tailing pond, stockpile, and mine facilities. For example, the tailing pond could be placed in the northwest (NW) area where the terrain shows low elevation (valleys) and minimal mineralization potential. However, the valley identified in the southwest (SW) corner of the contour map could also serve as a secondary option, as it offers natural containment and stability. Using natural low-lying areas (valleys) for the tailing pond reduces the need for extensive excavation and provides inherent structural stability. On the other hand, stockpiles should be in areas with moderate elevation and stable subsurface conditions. Thus, the central portion of Line 1 or Line 3 is ideal, as this area lacks metallic mineral deposits and offers accessibility while minimizing environmental and operational risks. Placing the stockpile on stable, non-mineralized terrain minimizes interference with future mining activities. Mine facilities were recommended to be placed on higher elevation terrain, such as the southeastern area, avoiding areas with high chargeability and resistivity anomalies indicating potential minerals. The hill in the southeast on the contour map is suitable for these facilities, ensuring stability and ease of monitoring. Establish mine facilities on elevated ground to ensure protection from flooding and to present an efficient site management. Further hydrological and environmental impact assessments are recommended to refine these placements.

CONCLUSIONS

In conclusion, the electrical resistivity imaging (ERI) survey in Keratong, Pahang, has successfully delineated subsurface geological features and identified zones with potential metallic mineral deposits. Key findings indicate

significant mineral presence at depths of 5 to 20 meters, particularly along survey Lines 2, 4, 5, 6, 7, and 8. These zones are recommended for targeted borehole drilling to validate and further explore the mineral potential.

Additionally, the northwest portion of the study area, characterized by low elevation and minimal mineralization potential, is suitable for establishing a tailing pond. Conversely, stockpiles and mine facilities should be located in geologically stable and non-mineralized regions specifically along Line 1 and 3 and on elevated terrain in the southeast. These site planning recommendations aim to optimize resource extraction, enhance operation efficiency, and minimizing environmental impacts and geotechnical risks.

ACKNOWLEDGEMENT

This study was supported by the Universiti Malaysia Pahang Al-Sultan Abdullah (Research grant number RDU243007 & PGR230318) and is highly appreciated. The authors further express their sincere gratitude to the anonymous reviewers for their constructive feedback, which has strengthened this manuscript.

AUTHORS CONTRIBUTION

MFI: Supervision, conceptualisation, investigation and methodology, writing-review & editing, validation. PII: Writing-original draft preparation. SD: Investigation, resources.

CONFLICT OF INTEREST

The authors declare no competing interest.

REFERENCES

- Al-Sudani, H.I.Z., 2019. Introduction to Surfer: Preliminary Training Course in Surfer Application in Contouring Mapping. https://www.researchgate.net/publication/331648966.doi:10.13140/RG.2.2.33827.50729.
- Arifin, M., Kayode, J., Izwan, M., Zaid, H., & Hussin, H., 2019. Data for the potential gold mineralization mapping with the applications of Electrical Resistivity Imaging and Induced Polarization geophysical surveys. Data in Brief, 22, 830-835.
- Bery, A.A., Saad, R., Mohamad, E.T., Jinmin, M., Azwin, I., Tan, N.M., & Nordiana, M., 2011. Electrical resistivity and induced polarization data correlation with conductivity for iron ore exploration. Electronic Journal of Geotechnical Engineering, 17, 3223 - 3337.
- Cook, R.H. & Suntharalingam, T., 1970. The geology and mineral resources of Pahang Tenggara (Sector "E" & "F"), Geol. Surv. Malaysia Ann. Rep. 1970, 104-116.
- Far, I.H., Kepic, A., & Javadipour, S., 2015. Resistivity and Induction polarization technique for mapping hematite rich areas in Iran. ASEG Extended Abstracts, 2015(1), 1-3. doi: 10.1071/ ASEG2015ab287.
- Ghoneim, S., Salem, S., & El-Wahid, K., 2022. Application of Remote Sensing Techniques to Identify Iron Ore Deposits in The Central Eastern Desert, Egypt: A Case Study at Wadi Karim and Gabal El-Hadid Areas. Arab J. Geosci., 15(1596), 1-12. doi:https://doi.org/10.1007/s12517-022-10871-3.
- Griffiths, D.H., & Barker, R.D., 1993. Two-dimensional resistivity imaging and modelling in areas of complex geology. Journal

- of Applied Geopyhsics, 29(3-4), 211-226.
- GuidelineGeo, 2012. ABEM Terrameter LS 2. Retrieved from GuidelineGeo: https://share.google/s3RU9yg7ODfo3SiBb. Date retrieved: 26 March 2024.
- Haldar, S., 2018. Mineral exploration: principles and applications. Elsevier, Cambridge. 370 p.
- Hutchison, C.C., & Tan, N.K., 2009. Geology of Peninsular Malaysia. Geological Society of Malaysia, Universiti Malaya, Kuala Lumpur. 107 p.
- Jones, F., 2018. Geophysics foundations: Physical properties: Electrical resistivity of geologic materials. UBC Earth and Ocean Sciences, https://www.eoas.ubc.ca/courses/eosc350/content/foundations/properties/resistivity.htm.
- Kearey, P., Brooks, M., & Hill, I., 2002. An Introduction to Geophysical Exploration 3rd ed. Blackwell Science Ltd., Oxford. 281 p.
- Layade, G.O., Ogunkoya, C.O., Makinde, V., & Ajayi, K., 2022. Application of 2D Electrical Resistivity Imaging for Mineral Ore Exploration With a Basement Complex Formation. Nigerian Journal of Basic and Applied Science, 29(1), 34-42.
- Loke, M., 1999. Electrical imaging surveys for environmental and engineering studies. Retrieved from www.abem.se. Date retrieved: 14 February 2024.
- Martínez-Pagán, P., Gómez-Ortiz, D., Martín-Crespo, T., Martín-Velázquez, S., & Martínez-Segura, M., 2021. Electrical Resistivity Imaging Applied to Tailings Ponds: An Overview. Mine Water and the Environment, 40(1), 285-297.
- Mielke, C., Muedi, T., Papenfuss, A., Boesche, N.K., Rogass, C., Gauert, C.D.K., Altenberger, U., & De Wit, M. J., 2016.
 Multi and hyperspectral spaceborne remote sensing of the Aggeneys base metal sulphide mineral deposit sites in the Lower Orange River region, South Africa. South African Journal of Geology, 119, 63 76.
- Misra, K., 1999. Understanding Mineral Deposit. Kluwer Academic Publisher, Washington. 861 p.
- Mohamed, K.R., & Abdullah, I., 1993. The occurrences of the oolitic limestone facies in the Semantan Formation. Warta Geologi, 19(4), 143-154.
- Nordiana, M.M., Rosli, S., Mokhtar, S.M., Nawawi, N.M., & Ismail, N.A., 2012. Imaging subsurface characterization at Bukit Bunuh using 2D resistivity method: the effectiveness of enhancing horizontal resolution (EHR) technique. International Journal of Environmental Science and Development, 3(6), 569-573.
- Parasnis, D.S., 2006. The electrical resistivity of some sulphide and oxide minerals and their ores. Geophysical Prospecting, 4(3), 249 278.
- Peng, L.C., Leman, M.S., Hassan, H., Nasib, B.M., & Karim, R., 2004. Stratigraphic Lexicon of Malaysia. Geological Society of Malaysia, Kuala Lumpur. 176 p.
- Pour, B. A., & Hashim, M., 2015. Structural mapping using PALSAR data in the Central Gold Belt, Peninsular Malaysia. Ore Geology Reviews, 64, 13-22.
- Said, U., 2002. Palynomorph assmblage from Keratong, Pahang: its age and emergence of angiospermlike pollen. Geological Society of Malaysia Annual Geological Conference 2002,

- May 26 27, Kota Bharu, Kelantan, Malaysia.
- Sajid, Z., Ismail, M., & Hanif, T., 2020. Mineralogical and geochemical imprints to determine the provenance, depositional history and tectonic settings of Triassic turbidites in the Semanggol and Semantan Basins, Peninsular Malaysia. Journal of Asian Earth Sciences, 203, 1-27.
- Sikah, J.N., Aning, A.A., Danuor, S.K., Manu, E., & Okrah, C., 2016. Groundwater exploration using 1D and 2D electrical resistivity methods. Journal of Environment and Earth Science, 6(7), 55-63.
- Syakir, M., Udin, W.S., Bahar, A.M., Fatihi, M., & Fikri, A., 2020. Alluvium assessment of gold-bearing layer in buried old river channel by using electrical resistivity method at Batu Melintang, Jeli, Kelantan. IOP Conference Series: Earth and Environmental Science, 549(2020), 012016. doi:10.1088/1755-1315/549/1/01201.
- Tan, S.N., Dan, M.F., Tonnizam, M.E., Saad, R., Madun, A., & Hazreek, Z.A., 2018. Interpretation of 2D resistivity with engineering. Journal of Physics: Conference Series, 995, 1-6.
- Wightman, W.E., Jalinoos, F., Sirles, P., & Hanna, K., 2004.
 Application of Geophysical Methods to Highway Related Problems. Federal Highway Administration, Lakewood. 744 p.
- Yamusa, I.B., Ismail, M.S., & Tella, A., 2021. Geospatial detection of hidden lithologies along Taiping to Ipoh streeth of the highway using medium resolution satellite imagery in Malaysia. Journal of Advanced Geospatial and Science Technology, 1(1), 19-37.
- Yang, C., Jia, H., Dong, L., Zhao, H., & Zhao, M., 2024. Selection of landsat-8 operational land imager (oli) optimal band combinations for mapping alteration zones. Remote Sensing, 16(2), 1-19. doi:https://doi.org/10.3390/rs16020392.
- Yixin, Y., Zhiyong, Z., Zelin, L., & Yong, Z., 2017. Three-dimensional resistivity and induced polarization data inversion with image focusing. In: Qingyun Di, Guo-qiang Xue & Jianghai Xia (Eds.), Technology and Application of Environmental and Engineering Geophysics: Selected Papers of the 7th International Conference on Environmental and Engineering Geophysics, ICEEG-Beijing 2016. Springer, Singapore. 283 p.
- Zaid, H., Arifin, M., Hussin, H., Basori, M., Umor, M., & Hazim, S., 2022. Manganese ore exploration using electrical resistivity and induced polarization methods in Central Belt, Peninsular Malaysia. Near Surface Geophysics, 20(6), 679-696.
- Zaid, H., Arifin, M., Kayode, J., Basori, M., Umor, M., & Hazim, S., 2023. Application of 2-D electrical resistivity imaging, and induced polarization methods for delineating gold mineralization at Felda Chiku 3, Kelantan, Malaysia. Sains Malaysiana, 52(1), 305-320.
- Zaini, M.S., Ishak, M.F., & Zolkepli, M.F., 2019. Forensic assessment on landfills leachate through electrical resistivity imaging at Simpang Renggam in Johor, Malaysia. IOP Conference Series: Materials Science and Engineering, 669(1), 1-7.
- Zaini, M.S., Ishak, M.F., Zolkepli, M.F., Wahap, M.S., Jaafar Sidek, J.I., Mohd Yasin, A., Zolkepli, M.N., Mohamad Sidik, M.H., Mohd Arof, K.Z., & Abu Talib, Z., 2020. Granite exploration by using electrical resistivity imaging (ERI): a case study in Johor. International Journal of Integrated Engineering, 12(8), 328-347.

Manuscript received 17 September 2024; Received in revised form 25 November 2024; Accepted 28 April 2025 Available online 28 November 2025